[CANCER RESEARCH 61, 8441–8447, December 1, 2001]

A New Noninvasive Approach in Breast Cancer Therapy Using Magnetic Resonance Imaging-guided Focused Ultrasound Surgery[1]

Peter E. Huber,[2] Juergen W. Jenne, Ralf Rastert, Ioannis Simiantonakis, Hans-Peter Sinn, Hans-Joachim Strittmatter, Dietrich von Fournier, Michael F. Wannenmacher, and Juergen Debus

Deutsches Krebsforschungszentrum (dkfz), Division of Radiation Oncology, D-69120 Heidelberg [P. E. H., J. W. J., R. R., I. S., J. D.]; Departments of Radiation Oncology [P. E. H., M. F. W., J. D.], Gynecology [H-J. S., D. V. F.], and Pathology [H-P. S.], University of Heidelberg Medical School, D-69120 Heidelberg, Germany

ABSTRACT

An ideal vision of modern medicine includes tumor surgery with the human body remaining completely intact. A noninvasive therapy could avoid infections and scar formation; it would require less anesthesia, reduce recovery time, and possibly also reduce costs. This study investigated whether human breast cancer can be effectively treated with a novel combination of image guidance and energy delivery, noninvasive magnetic resonance imaging (MRI)-guided focused ultrasound (FUS). We have developed a FUS therapy unit guided by MRI for the treatment of human breast tumors in a clinical 1.5 T MR scanner. With interactive target segmentation on MRI, defined volumes could be noninvasively treated in a single session with on-line MR temperature control. The ultrasound waves were focused through the intact skin and resulted in the localized thermal tissue ablation at a maximum temperature of 70°C. The therapy principle was first demonstrated in sheep breast *in vivo* and was then applied in a patient with core biopsy-proven invasive breast cancer 5 days before breast-conserving surgery. MRI proved suitable to delineate the breast cancer, served as stereotactic treatment planning platform, and delineated the FUS-related tissue changes such as interruption of tumor blood flow. Furthermore, MRI localized the hot spot in the tumor and measured temperature elevation during the treatment. This allowed us to monitor the efficacy and safety of FUS therapy. Immunohistochemistry of the resected specimen demonstrated that FUS homogeneously induced lethal and sublethal tumor damage with consecutive up-regulation of p53 and loss of proliferative activity. This effect was realized without anesthesia and damage to the surrounding healthy tissue or systemic effects. Overall, our results show that noninvasive MRI-guided therapy of breast cancer is feasible and effective. Thus, MRI-guided FUS may represent a new strategy for the neoadjuvant, adjuvant, or palliative treatment in selected breast cancer patients and in patients with other soft-tissue tumors.

INTRODUCTION

Breast cancer is the most frequently occurring malignant disease in women with a lifetime risk of ~1:8 to 1:10 in the United States of America (1). Mastectomy, introduced by William Halstedt in 1894, was the mainstay of therapy for ~80 years (2, 3). The clinical impetus and ethical justification for pursuing less invasive therapies to improve cosmesis have derived from the success of BCT[3] in combination with adjuvant treatment modalities such as radiotherapy, chemotherapy, and hormonal therapy since the 1970s (4).

Although BCT is not a major procedure, it is invasive and cosmetically undesirable in some patients. Furthermore, some patients with concomitant diseases, or elderly patients, can be precluded from being surgical candidates.

A completely noninvasive local therapy would require less anesthesia, would reduce recovery time, could avoid infections and scar formation, and possibly also reduce cost (5). This ideal of noninvasive therapy can be realized, if two prerequisites are fulfilled. First, imaging technology must provide accurate information on the exact anatomy of the tumor and the surrounding healthy tissue. Second, energy must be precisely delivered to the target (6). In recent years, a variety of minimally invasive therapies have been applied to breast tumors including interstitial laser coagulation, radiofrequency, cryotherapy, and interstitial radiotherapy (7).

These techniques, however, still require a probe to be inserted. By contrast, percutaneous focused ultrasonic waves have the potential to very precisely deliver energy to a given point in soft tissue within an accuracy of 1 mm through the intact skin (8). The ultrasound energy can induce temperature elevations of 55°C to 90°C at the focal spot in less than 10 s and instantaneously induce cellular death and vascular obliteration in normal and tumor tissue (8–10). Because of the steep thermal gradients, the boundaries of the ultrasound-affected volumes are sharply demarcated (8). To treat a larger area, the focal spots can be closely spaced until the entire target is covered (10). Although the potential of FUS has been tested in a variety of tumors, including brain tumors, beginning more than 50 years ago (11–14), clinical acceptance has been lacking because of (*a*) the lack of radiological and computational techniques for controlling the focal spot position; (*b*) a lack of precise target definition; (*c*) the unavailability of beam temperature dosimetry; and (*d*) the sparseness of clinical outcome data.

Interest in FUS therapy has been revived especially in combination with emerging MRI technology (15), because MRI is the method of choice for accurate delineation in many tumors including breast tumors (16, 17), and, moreover, MRI can noninvasively measure the ultrasound-induced temperature, because several MRI parameters are temperature dependent (18–21). Thus, the combination of both MRI and FUS simultaneously allows the definition of tumor margins, the noninvasive thermal therapy, and the on-line control of the current therapy site by thermal MRI. Additionally, it has been shown in animal studies that the FUS-treatment effect could be judged by T1w i.v. contrast MRI directly after therapy as an interruption of blood perfusion (19–23). In recent years, the technical feasibility of conducting FUS therapy guided by MRI has been demonstrated and improved in terms of accurate and fast temperature control in *ex vivo* tissue and animal studies *in vivo* (18–20, 22–25), including a recent pilot study in benign fibroadenoma in the human breast (26).

The objective of the present study was to transfer MRI-guided FUS technology from animal studies to noninvasive treatment of human breast cancer. We have developed and tested a FUS therapy unit with thermoimaging by MRI in sheep and then applied 5 days preoperatively in a human breast cancer patient. We show (*a*) the feasibility of performing accurate MRI-based FUS therapy planning; (*b*) the feasibility of noninvasive on-line temperature mapping in the tumor by MRI while performing FUS; (*c*) the localized interruption of blood

Received 5/24/01; accepted 10/1/01.

The costs of publication of this article were defrayed in part by the payment of page charges. This article must therefore be hereby marked *advertisement* in accordance with 18 U.S.C. Section 1734 solely to indicate this fact.

[1] Supported by the German Research Foundation (DFG) Grant Hu 798/1-3 and a grant from the Helmholtz Society.

[2] To whom requests for reprints should be addressed, at German Cancer Research Center/Deutsches Krebsforschungszentrum (dkfz), Division of Radiation Oncology, Im Neuenheimer Feld 280, D-69120 Heidelberg, Germany. Phone: 49-6221-42-2448; Fax: 49-6221-42-2514; Email: p.huber@dkfz-heidelberg.de.

[3] The abbreviations used are: BCT, breast-conserving therapy; FUS, focused ultrasound; MR, magnetic resonance; MRI, MR imaging; T1w, T_1-weighted; T2w, T_2-weighted; ER, estrogen receptor; PR, progesterone receptor.

perfusion in healthy and tumor tissue by FUS; and (*e*) the ability of FUS to accurately and thoroughly induce tumor cytotoxicity as planned on MRI.

MATERIALS AND METHODS

FUS Therapy Unit. All of the parts of the MRI-guided FUS unit for the animal experiments and the human breast were constructed of nonmagnetic materials to be compatible in the 1.5 T magnetic field of a clinical MR tomograph (Magnetom Vision Plus; Siemens, Erlangen, Germany). The human ultrasound applicator accommodated the breast with a bowl-shaped indentation, whereas the physical ultrasound transducer characteristics remained identical compared with the animal set-up. The remote-controlled therapy unit consisted of an ultrasound source, a MRI coil, and a hydraulically driven positioning system. A central workstation controls the operational status including power, ultrasound transducer motion, and position (Fig. 1).

The ultrasound transducer (focal distance, 68 mm; center frequency, 1.7 MHz) is mounted on a positioning system behind an ultrasound transparent window inside the breast indentation. The computer-controlled positioning system is based on three linear actuators. These extensible links consist of hydraulically driven linear stepper motors, supplied by short pressure pulses that are transformed into precise steps of 0.1 mm. Photoelectric barriers, mediated by fiber optics, control the steps, which results in a mechanical accuracy of the ultrasound focusing system better than 1 mm.

The focus of the ultrasound source, the therapeutically effective area, is cigar-shaped, has a diameter of ~1.1 mm and a length of 8.7 mm. This value had been determined in independent *in vivo* studies. During MRI planning and FUS therapy, the breast is placed on the transparent window surrounded by the MR coil (Fig. 1). To optimize the ultrasound beam angle, the sonication window can be adjusted around a vertical axis through the center of the breast. Acoustic coupling is mediated by ultrasound coupling jelly and water.

MRI for Therapy Planning, Monitoring, and Thermometry. The objective of MRI-based therapy planning was to calculate an optimized beam pattern covering the entire target area in such a manner that the multiple focal ultrasound volumes were packed until the entire target volume was treated.

For therapy planning, T2w images turbo spin echo were taken to define the target volume [repetition/echo/acquisition time (TR/TE/TA), 4500 ms/99 ms/103 s; slice thickness (TH), 3 mm]. Additionally, native T1w three-dimensional flash images (TR/TE/TA, 20 ms/4 ms/145 s; TH, 3 mm) with a high spatial resolution were acquired as an additional anatomical baseline. These T2w sequences were also performed every 10 min during the treatment to monitor potential edema development, and the T1w sequences were also used directly after completing the treatment to analyze perfusion changes after i.v. administration of the paramagnetic contrast agent gadolinium (Prohance; Bracco-Byk Gulden, Konstanz, Germany; dose, 0.2 ml/kg).

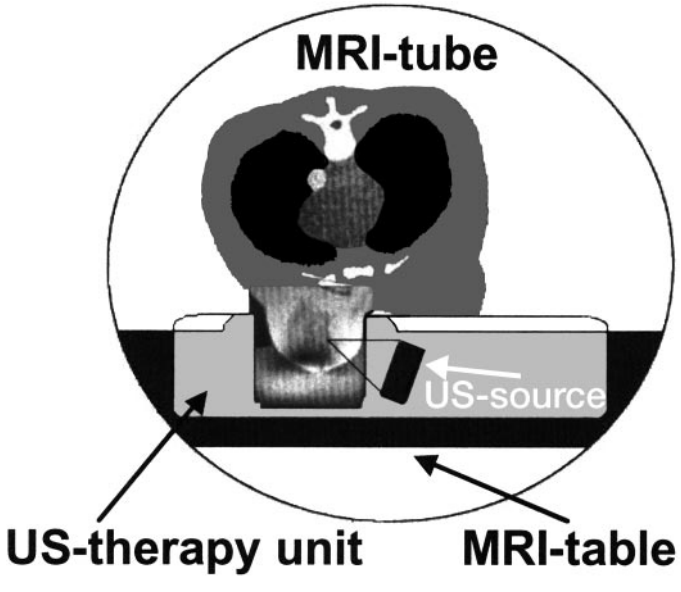

Fig. 1. Principle of MRI-guided FUS therapy: FUS penetrates through the intact skin to volumes with dimensions of 10–20 mm^3 and induces temperatures of 55°C to 90°C in the focal spot in less than 10 s. The target volume is outlined in MRI. A close spacing of individual small foci results in overlapping treatment zones that cover the entire target volume. The MRI-guided FUS system consists of a supply unit for radio frequency conditioning, driving hydraulics, the cooling and fluidic system, MR-compatible ultrasound applicator including a therapeutic ultrasound transducer with a hydraulically driven positioning system and coil for MRI within the MR scanner and computers for therapy planning, MRI-based temperature monitoring, and MRI.

Therapy planning calculations were based on tumor size, the length of the ultrasound pathway measured by MRI. Treatment planning coordinates of the MRI measurements were correlated with the coordinate system of the ultrasound therapy unit by using MR-visible markers attached to the ultrasound applicator. Target definition and segmentation were adapted from three-dimensional radiotherapy with ionizing radiation referred to as "stereotactic conformal radiotherapy." In contrast to conventional stereotactic radiotherapy, the *X*, *Y*, and *Z* axes of the FUS coordinate system were not fixed to the MRI table, but attached to the flexible ultrasound therapy applicator.

To monitor the induced temperature elevation, during each sonication, temperature-sensitive T1w Saturation-Recovery-TurboFLASH (SRTF) images were used [TR/TE/TA, 10.2 ms/4 ms/6 s; recovery time (T_{REC}), 1100 ms; excitation angle α, 12°; number of slices, 3; TH, 5 mm; acquisition matrix (MA), 128 × 128; field of view (FOV), 200 × 200–300 × 300 mm^2]; three parallel slices covering the focus region and the adjacent structures were displayed (21, 22). The first slice was started 2 s before the end of sonication; the second immediately after; and the third slice, 2 s after sonication. Temperature maps were calculated on line using the temperature-related signal reduction with respect to reference images acquired before sonication. MRI temperature accuracy and calibration were evaluated in *ex vivo* muscle tissue and in *ex vivo* sheep mammary glands by using fiber optic probes and thermocouples (21). The T1w temperature imaging was used, because these MR sequences also exhibit reliable temperature-dependent signals in fatty tissue that is especially typical in the breast cancer population of the elderly (21).

Animal Model. All of the animal experiments and animal care were conducted in accordance with the guidelines of the Federal Government of Germany and were approved by institutional laws and governmental committees. Eight female sheep weighing between 60 and 80 kg were selected as the animal model for the postmenopausal human female breast. Each sheep udder was treated twice at different sites with FUS at an interval of 4 weeks between the two treatments to analyze early and late tissue effects. One of the two lobes of the breast was chosen for each treatment session. To facilitate acoustic coupling, the wool over the target region was sheared and the skin was depilated (Pilca; Schwarzkopf & Henkel, Düsseldorf, Germany).

The animals received two i.m. injections of 20 mg of xylazine 2% (Rompun; Bayer, Leverkusen, Germany) as a premedication. Anesthesia was initiated by an i.v. injection of disoprivan 1% (Zeneca, Plankstadt, Germany) at a dose of 3–5 mg/kg body weight. After intubation, anesthesia was sustained by inhalation of 1.5% halothane (Fluothane; Zeneca, Plankstadt, Germany) in pure oxygen. The respiration frequency was reduced to 7/min for triggering the start of the MR temperature imaging. Thus, MRI was performed 2 s before the end of the 9-s sonication phase, while respiration was stopped for the time needed to acquire the MR image. For therapy planning, baseline T2w images were obtained and geometrically well-defined target volumes in the healthy sheep breast were outlined on the MR image. During treatment, the animals were provided with a balanced electrolyte solution (Sterofundin; Braun, Melsungen, Germany). Four h after the second treatment, the sheep were killed and the organs were resected and stored in 4% formaldehyde. Tissue slices were cut perpendicular to the path of sound propagation. Histological cross-sections, 3–5-μm thick, were taken at 5-mm intervals throughout the entire udder and conventionally stained with H&E.

Clinical Study. The treatment protocol was designed with the strict understanding of not compromising the patient's oncological prognosis as well as for facilitating a pathological analysis of the tissue effects induced by ultrasound. The new noninvasive treatment method using FUS was given in addition to the standard treatment. Therefore, the ultrasound procedure was scheduled as a neoadjuvant approach that preceded the open surgical removal of the tumor followed by the prescribed adjuvant therapies. The study was approved by the

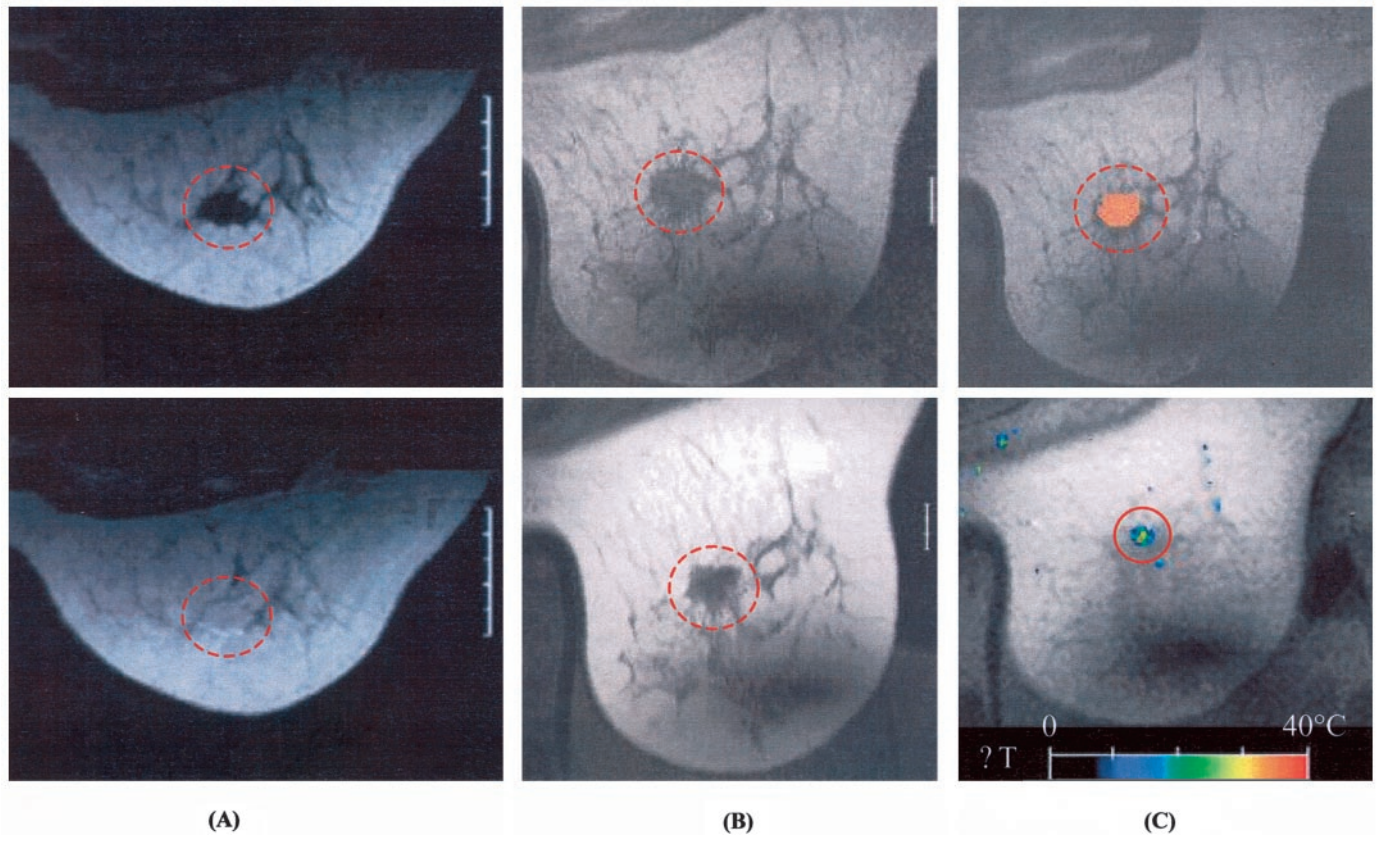

Fig. 2. *A*, T1w MRI mammography of a biopsy-confirmed breast cancer in a standard breast coil 2 days before ultrasound therapy, without i.v. contrast (*top*) and after i.v. contrast (*bottom*), showing strong tumor contrast enhancement. *B*, T1w MR images in the ultrasound treatment unit: immediately before, *i.e.*, without i.v. contrast (*top*), and after therapy with i.v. contrast (*bottom*), exhibiting a complete lack of contrast enhancement after FUS therapy. *C*, T2w MRI treatment planning with definition of 80 foci (*top*) and MRI thermometry during sonication with color-coded temperature distribution after treatment (*bottom*).

local Ethics Committee as a prospective nonrandomized one-arm study. Written informed consent was obtained before the beginning of therapy.

The reported breast cancer patient was a 56-year-old menopausal female who was otherwise in good health. She was a typical candidate for breast-conserving surgery. On H&E-stained sections of a cut-core biopsy, the tumor was classified as an invasive ductal carcinoma, grade 2, with positive ER and PR status (27). Additionally, standard MRI mammography conducted 2 days before FUS treatment revealed the tumor to be a well-circumscribed mass of $2.2 \times 2 \times 1.4$ cm^3 (Fig. 2*A*) that was located in the central part of the right breast.

Exclusion criteria were extensive intraductal components (EIC), extensive mammographic calcifications, multicentric disease and prior local therapies, chemotherapy, or hormonal therapy. Adjuvant therapy decisions were intended to be based on the core biopsy results along with the open surgery and dissection of the axillary lymph nodes.

Before ultrasound therapy, the patient was given only 5 mg of diazepam as an oral sedative, and no other general or local anesthesia was administered during the entire procedure.

The open surgery was performed as standard breast-conserving-surgery procedure 5 days after ultrasound therapy. The specimen obtained after the surgery was fixed in buffered formalin for 18 h and worked up topographically (27, 28). Immunohistochemistry was performed at the core biopsy before FUS and from one representative paraffin block of the tumor after FUS. We used the Techmate 500 immunohistochemistry system (all of the reagents from Dako, Copenhagen, Denmark) and the following primary monoclonal antibodies (clones in parentheses): Ki67 (MIB-1); HER-2/neu (A0485); p53 (DO7); bcl-2 (124); ER (1D5); and PR (PR88).

RESULTS

MRI Temperature Measurement during FUS. MRI-based noninvasive thermometry was performed during each 9-s sonication across the focal plane in both the animal and the human studies. The temperature maps and. thus, the spatial coordinates of the actual ultrasound focus were calculated on line and were displayed in a color-coded representation. Image acquisition, data transfer, and calculation of the temperature measurements were realized within 10 s, allowing the temperature maps to be evaluated before the next ultrasound pulse was applied. The maximum temperature detected in the sheep breast and the human breast cancer were $\sim$70°C $\pm$ 5°C. The individual temperature resolution for a single sonication was $\sim$2°C –3°C when compared with invasive temperature probes in independent experiments. The spatial accuracy of the temperature localization was better than 2 mm, depending on the MRI resolution. The temperature map was also superimposed on the T2w baseline therapy planning image to visualize potential patient movements during therapy.

Animal Study. The sheep breast was used as an *in vivo* model, because the sheep udder resembled the human breast in size, geometry, and physical characteristics.

Aside from temperature monitoring inside the sheep breast after each ultrasound pulse (maximum, 70°C $\pm$ 5°C), T2w images taken every 10 min exhibited increasingly hyperintense, poorly demarcated regions that suggested a mild localized edema in the target area. Postcontrast T1w images, taken immediately after completing the 1–2-h long ultrasound therapy, exhibited hypointense regions suggesting complete interruption of blood flow. The L-shape and the size of the predefined MRI planning target volumes agreed well with the nonperfused regions (median, 1190 mm^3 *versus* 1310 mm^3; range, 400-1810 mm^3 *versus* 320-2490 mm^3) after therapy. Pairwise Student's t test revealed a nonsignificant difference ($P > 0.7$) between the individual MRI planning sizes and their treatment outcome, which

was determined by MRI as hypointense nonperfused regions with a high correlation (Pearson's test, r, 0.88; $P = 0.001$).

The histological analysis of the acute effects 4 h after therapy revealed edematous swelling, hyperemia, and mild lymphoplasmacellular infiltration of the stroma. Histological samples taken 3 days and 4 weeks, respectively, after ultrasound therapy yielded a homogeneous-shaped necrosis. The dimensions of the necroses (median, 1050 mm^3; range, 350-1750 mm^3) correlated well with the hypointense nonperfused regions on MRI directly after FUS (Pearson test, r, 0.82; $P = 0.001$) with a nonsignificant difference between necrosis and MRI size (pairwise Student's test, $P > 0.6$). This indicated that the nonperfused region was lethally damaged.

No unexpected treatment-related side effects were detected. Especially noteworthy, the skin over the treated region remained unaffected. The animal study confirmed that, based on MRI planning, geometrically well-defined lesions could be noninvasively induced in sheep breast with the FUS treatment unit developed by us. Therefore, we decided to start a clinical phase I/II study in human breast cancer patients.

MRI-guided FUS of Human Breast Cancer. After positioning our first patient to be treated with FUS in the MR scanner, T1w and T2w MR images of the breast perpendicular to the plane of ultrasound propagation were taken as an anatomical baseline and for therapy planning calculations (Fig. 2). In agreement with the standard MRI mammography conducted 2 days before ultrasound therapy, the treatment coil visualized the tumor ($2.2 \times 2 \times 1.4$ cm^3) in the central part of the right breast.

For treatment planning, the target volume was outlined with a 1–2-mm rim inside the MRI visible tumor boundaries in an effort to facilitate the pathological analysis of the therapeutic ultrasound effects and their distribution completely within the tumor boundaries (Fig. 2). These MR images also proved the absence of air bubbles in the ultrasound pathway. The optimized calculations for covering the planning volume yielded 80 single ultrasound pulses of 9 s each at 30–50 W acoustic power. A 13-s interval was added between each single pulse to prevent a marked temperature elevation in healthy adjacent tissue as a result of potential heat accumulation along the ultrasound pathway from the skin to the tumor. This interval was further extended to 20–50 s to conduct temperature-sensitive MRI for each single thermal spot.

The MRI temperature monitoring enabled us to compare the actual heat focus position with the planned focus position in the planning image and, thereby, to exclude any patient movements that might have occurred during the 1.5 h-long procedure. As an additional noninvasive therapy monitoring, T2w MR imaging was performed every 20 ultrasound pulses. As an acute therapy-related effect, the images revealed a slightly growing signal hyperintensity in the tumor region suggestive of mild edema, which thereby independently verified correct targeting.

Immediately after the therapeutic sonications had been completed, the extent of the therapeutic effect on the tumor vasculature was evaluated by T1w MR images after the i.v. application of gadolinium. The hypointense, sharply demarcated area with a hyperintense boundary zone revealed an absence of contrast agent in the treated area, which suggested a complete interruption of blood perfusion with a hypervascularized rim (Fig. 2*B*). This treated area corresponded well with the outlined region on the pretherapy MR images.

Directly after finishing the ultrasound therapy session and until 3 months thereafter, including the adjuvant radiotherapy, the skin over the treated area did not exhibit any ultrasound-related visible changes, and the patient did not show any local or systemic symptoms. Despite the absence of anesthesia, the patient did not experience pain or discomfort during or after FUS therapy with the exception of a mild pressure sensation in the tumor region during each 9-s sonication.

Five days after ultrasound therapy, the open surgical treatment was performed as a standard procedure, including breast-conserving surgery and axillary lymph node dissection. A visual inspection was unable to detect any adverse effects in normal tissue, including the skin. The tumor region appeared softer when compared with the usual intraoperative appearance of breast cancer, which suggested a possible method of differentiation from the surrounding healthy tissue.

The work-up of the resection specimen revealed a 2.2-cm well-demarcated breast tumor with negative margins, as well as negative axillary lymph nodes. The adjuvant treatment modalities prescribed to this patient included, therefore, local radiotherapy and hormonal therapy with tamoxifen, which was the same as it had been without FUS-pretherapy. On the cut surface, a 1–2-mm hyperemic rim was visible in the tumor periphery (Fig. 3*A*). This rim corresponded well with the target outlined in the MRI planning image and with the hyperintense rim surrounding the nonperfused inner zone on T1w MRI that was taken immediately after therapy. Accordingly, microscopy identified the rim zone as vital tumor tissue with congested capillaries and hemorrhaging. In the outlined, treated part of the tumor, tumor cells were partially necrotic, as confirmed by the lack of nuclear staining, and mostly sublethally damaged with chromatin clumping. The spatial accuracy of the noninvasive image-guided tumor destruction was 1–2 mm based on the MR coordinates along with the pathological analysis. This value was in accordance with the results from the sheep experiments.

Furthermore, we evaluated the effect of ultrasound therapy on the breast cancer hormone receptor status and cellular proliferation. The immunohistological stains on the cut-core biopsy, taken before ultrasound, revealed strong staining for ER and PR (in 100% of the tumor cells) and bcl-2 as well as moderate proliferative activity. Additionally, p53 was detectable in 30% of the tumor cells before ultrasound and HER-2/neu was negative. In contrast, after ultrasound, ER and PR were consistently negative, Ki67 was only 5% and p53 was up-regulated with up to 90% of the tumor cell nuclei in the ultrasound-treated area of the tumor being positive (Fig. 3, *B* and *C*). Interestingly, the proliferative activity was also reduced in the 1–2-mm rim zone beyond the segmented area on MRI planning images. These differences in staining patterns were a consequence of the ultrasound treatment and reflect the sublethal-to-lethal tumor damage with a subsequent up-regulation of p53 and loss of proliferative activity as well as positive receptor status. In the adjacent tissue, no treatment-related effects could be detected in the pathological specimen taken after resection.

DISCUSSION

An ideal vision of modern medicine includes instantly effective tumor therapy with the human body remaining completely intact. It has been proposed that noninvasive therapy of breast cancer without opening the skin can be achieved by the combination of image guidance and novel forms of energy delivery (5–7). In the current feasibility study, we show that human breast cancer can be effectively treated with noninvasive FUS thermal therapy in a single treatment session using MRI planning and MRI on-line thermometry without marked side effects. Our results also show that an interruption of tumor blood flow can be induced by FUS as measured by MRI. The consequence of the FUS therapy is homogeneous lethal and sublethal tumor damage with subsequent up-regulation of p53 and loss of proliferative activity. Furthermore, the results demonstrate the advantage of combining noninvasive FUS with MRI in breast cancer. First, MRI is suitable to delineate the gross tumor extent, can serve as

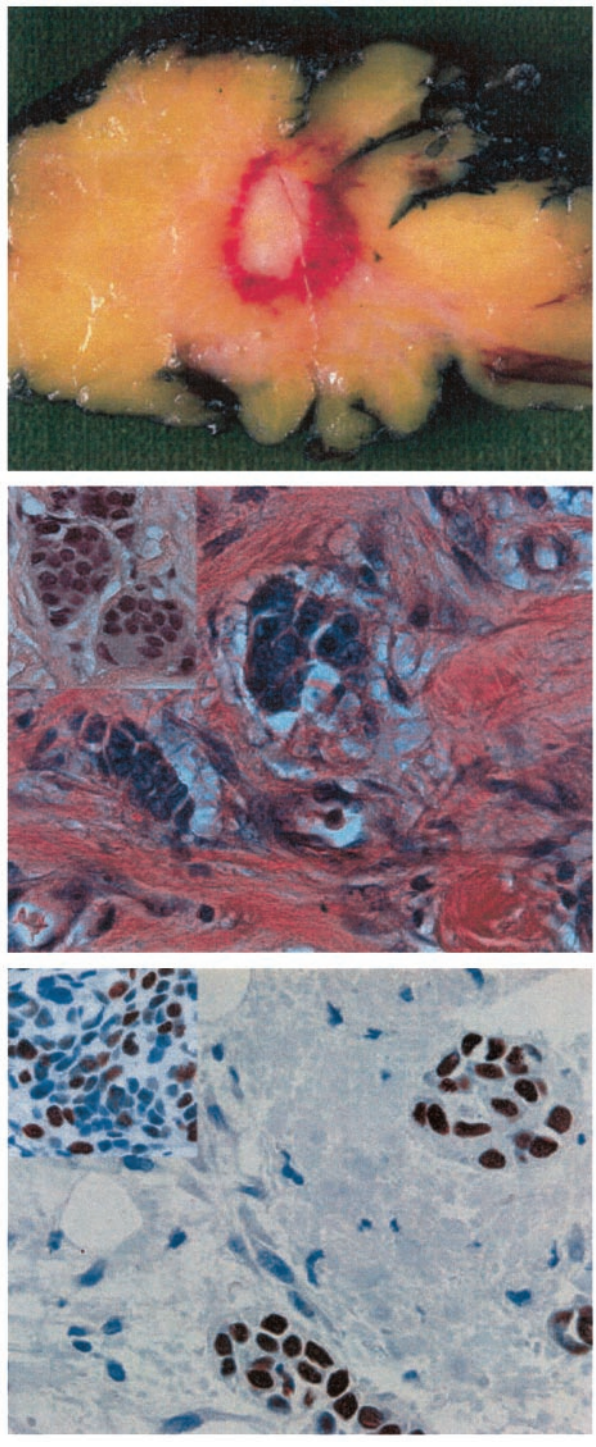

Fig. 3. Macroscopic specimen 5 days after focused ultrasound. *A*, pathological slice of the target region, cut perpendicular to the direction of ultrasound propagation. White area with a hyperemic rim, the treated target. *B*, microscopic specimen: high-power view of vital and degenerating tumor cells (H&E stain; ×400) after ultrasound therapy. *Inset*, the pretherapy status in the core biopsy. *C*, microscopic specimen: p53 stain of the tumor center containing two clusters of tumor cells with p53 overexpression within necrotic cell debris (×400). *Inset*, the pretherapy status in the core biopsy.

stereotactic treatment platform for FUS therapy, and is suitable for delineating the FUS related changes in the breast. Second, and maybe more important, MRI is suitable for localizing the hot spot in the tumor and measuring temperature elevation during the treatment. This feature allows monitoring the efficacy and safety of FUS therapy.

Here, we have developed and tested a FUS therapy unit under T1w thermoimaging with MRI for the treatment of human breast tumors in a clinical 1.5 T MR scanner. The ultrasound waves were focused through the intact skin and resulted in the localized thermal (maximum, ~70°C) therapy of tissue. With this treatment unit, it is possible to treat defined volumes based on interactive target segmentation of MR planning images with on-line MR temperature control. The tissue effects of the single-focus ultrasound therapy unit were first tested and analyzed in an experimental series using sheep breast *in vivo* and then transferred to a patient with core-biopsy-proven invasive breast cancer. In the patient, who was a candidate for BCT, the MRI-guided FUS procedure was scheduled as a neoadjuvant approach that preceded the open surgical removal of the tumor and the appropriate adjuvant therapies.

In this article, we have described what is, to our knowledge, the first report of MRI-guided FUS in a malignant tumor in humans. It follows a series of technical and animal studies (18–25) and one recent report of treating benign fibroadenomas in the breast (26).

Although localized heat induction is considered the prominent tissue effect of the type of FUS therapy used in the present study, it was not determined here whether the tumor cytotoxicity was directly heat induced or secondary to the interruption of blood flow, or a combination of both factors. Interactions of ultrasound with biological tissues are, in general, dependent on the acoustic parameters such as peak pressure amplitude and intensity. Therapeutic ultrasound can induce nonthermal mechanical, cavitational, and the better-defined temperature effects. In previous studies, we and others have shown that all of these interaction mechanisms can have antitumor effects *in vivo* (9, 10, 14, 20, 29–32). At the microscopic level, it has also been shown in recent reports that ultrasound can induce apoptosis *in vitro*, presumably via cavitation (33), and in animals *in vivo* via heat induction (34). Moreover, ultrasound waves have been reported to make cell membranes permeable and show promise as a gene-transfer methodology (35–36). Therefore, a combination of different mechanisms could be involved in the lethal and sublethal tumor damage with loss of proliferative activity, p53 up-regulation, and loss of receptor positivity observed here. Furthermore, we had not expected an up-regulation of p53 in breast cancer after the necroses seen in the sheep study, especially with the same maximal temperature of 70°C that was equally induced in animal and human tissue. Whereas the maximal temperature measured corresponds well with the short δ-like peak of thermal energy delivery, variable physiological conditions such as tissue type and local perfusion could explain slightly different biological reactions, especially in between the foci. Although the therapy regimen used in the patient was sufficient to homogeneously induce tumor cell death, a tighter scanning pattern of the ultrasound foci, higher intensity, or longer sonication per pulse might enhance the instantaneous antitumor effect in breast cancer. This issue of optimal dosing has to be addressed further.

The local management of invasive breast cancer has long been the domain of the surgeon alone. Today, treatment involves a collaborative effort of surgery, radiology, pathology, radiation therapy, and medical oncology (3). MRI-guided FUS as a localized procedure could potentially benefit patients by downstaging the disease and facilitating a potentially higher rate of breast-conserving procedures, similar to neoadjuvant chemotherapy (3, 37–39), but without the chemotherapy inherent systemic side effects. Alternatively, MRI-guided FUS can support breast-conserving surgery by assisting in the presurgical definition of the tumor boundaries that may result in more precise surgery and in a reduction of the breast tissue volume that must be surgically removed. This can result in less shape distortion and better cosmesis. Finally, MRI-guided FUS therapy has the potential to replace open surgery in breast cancer patients in carefully

selected cases, such as patients with high operative risks, elderly patients, or patients not willing to undergo surgery.

Advantageous to MRI-guided FUS is that the breast is readily accessible to ultrasound and can be easily immobilized. Additionally, MRI is a sensitive and the most accurate imaging method for breast cancer when compared with the pathological specimen itself (16, 17). In contrast, a permanent disadvantage of noninvasive MRI-based tumor therapy is that MRI is unlikely to adequately delineate the extent of microscopic tumor disease and, therefore, cannot fully replace histological examination. Instead, there may be cases in which MRI-guided FUS may interfere with a full pathological examination of a specimen. Other potential disadvantages include the lack of improving tumor control or the addition of cost.

Aside from the breast, possible other target sites for FUS include organ systems that are accessible to diagnostic ultrasound devices, such as the head and neck, kidney, liver, and prostate. In contrast to alternative minimally invasive treatment methods (such as laser-induced, interstitial thermotherapy; RF ablation; or cryosurgery), FUS is noninvasive and does not require that a probe be inserted (7, 40–42). This leads to spatial flexibility, and the stereotactic treatment-planning principle guarantees high spatial accuracy of the focal position within ~1–2 mm.

With respect to future clinical applications of MRI-guided FUS, technical challenges remain. Most notably, tumor imaging, organ movement during therapy, and delivery of sufficient thermal dose throughout the target within a minimum amount of time are areas for potential improvements. These goals can be approached by both MRI technology, including options for molecular imaging (43), and improvements in ultrasound technology (44), such as phased arrays (45, 46). We believe that noninvasive image-guided therapies have the potential to change the treatment paradigm in selected cancer patients with neoadjuvant, adjuvant, or palliative intention. Ultimately, however, the clinical roles of such therapies must be defined in large trials.

ACKNOWLEDGMENTS

We thank Siemens Corporation (Erlangen, Germany), especially Dr. Arnulf Oppelt, and EDAP/TMS Corporation (Lyon, France) for continuous support.

REFERENCES

1. Landis, S. H., Murray, T., Bolden, S., and Wingo, P. A. 1999 cancer statistics. CA Cancer J. Clin., *49:* 8–31, 1999.
2. Halstedt, W. S. The results of radical operations for the cure of carcinoma of the breast. Ann. Surg., *66:* 1–9, 1907.
3. Morrow, M., and Harris, J. R. Local management of invasive breast cancer. *In:* J. R. Harris, M. E. Lippmann, M. Morrow, M., and L. K. Osborne (eds.), Diseases of the Breast, pp. 515–560. Philadelphia: Lippincott, 2000.
4. Fisher, B., Redmond, C., Poisson, R., Margolese, R., Wolmark, N., Wickerham, L., Fisher, E., Deutsch, M., Caplan, R., Pilch, Y., *et al*. Eight year results of a randomized trial comparing total mastectomy and lumpectomy with or without irradiation in the treatment of breast cancer. N. Engl. J. Med., *320:* 822–828, 1989.
5. Rattner, D. W. Future directions in innovative minimally invasive surgery. Lancet, *353* (Suppl. 1)*:* 12–15, 1999.
6. Jolesz, F. A. Image-guided procedures and the operating room of the future. Radiology, *204:* 601–612, 1997.
7. Hall-Craggs, M. A. Interventional MRI of the breast: minimally invasive therapy. Eur. Radiol., *10:* 59–62, 2000.
8. ter Haar, G. Ultrasound focal beam surgery. Ultrasound Med. Biol., *21:* 1089–1100, 1995.
9. Hill, C. R., and ter Haar, G. R. Review article: high intensity focused ultrasound—potential for cancer treatment. Br. J. Radiol., *68:* 1296–1303, 1995.
10. Gelet, A., Chapelon, J. Y., Pangaud, C., and Lasne, Y. Local control of prostate cancer by transrectal high intensity focused ultrasound therapy (HIFU): preliminary results after 113 procedures in 50 patients. J. Urol., *161:* 156–162, 1999.
11. Lynn, J. G., Zwemer, R. L., Chick, A. J., and Miller, A. E. A new method for the generation and use of focused ultrasound in experimental biology. J. Gen. Physiol., *26:* 179–193, 1942.
12. Fry, W. J., Barnard, J. W., Fry, F. J., Krumins, R. F., and Brennan, J. F. Ultrasonic lesions in the mammalian central nervous system. Science (Wash. DC), *122:* 517–518, 1955.
13. Lele, P. P. A simple method for production of trackless focal lesions with focused ultrasound: physical factors. J. Physiol., *160:* 494–512, 1962.
14. Heimburger, R. F. Ultrasound augmentation of central nervous system tumor therapy. Indiana Med., *78:* 469–479, 1985.
15. Hynynen, K., Darkazanli, A., Unger, E., and Schenck, J. F. MRI-guided noninvasive ultrasound surgery. Med. Phys., *20:* 107–115, 1993.
16. Boetes, C., Mus, R. D., Holland, R., Barentsz, J. O., Strijk, S. P., Wobbes, T., Hendriks, J. H., and Ruys, S. H. Breast tumors: comparative accuracy of MR imaging relative to mammography and US for demonstrating extent. Radiology, *197:* 743–747, 1995.
17. Mumtaz, H., Hall-Craggs, M. A., Davidson, T., Walmsley, K., Thurell, W., Kissin, M. W., and Taylor, I. Staging of symptomatic primary breast cancer with MR imaging. Am. J. Roentgenol., *169:* 417–424, 1997.
18. Chung, A. H., Jolesz, F. A., and Hynynen, K. Thermal dosimetry of a focused ultrasound beam *in vivo* by magnetic resonance imaging. Med. Phys., *26:* 2017–2026, 1999.
19. Graham, S. J., Chen, L., Leitch, M., Peters, R. D., Bronskill, M. J., Foster, F. S., Henkelman, R. M., and Plewes, D. B. Quantifying tissue damage due to focused ultrasound heating observed by MRI. Magn. Reson. Med., *41:* 321–328, 1999.
20. Huber, P., Stepanow, B., Debus, J., Jöchle, K., Mory, M., Jenne, J., Werner, A., van Kaick, G., and Lorenz, W. J. Temperature monitoring of focused ultrasound therapy by MRI. IEEE Ultrasonics Symp. Proc., *13:* 1825–1828, 1995.
21. Bohris, C., Schreiber, W. G., Jenne, J., Rastert, R., Spoo, J., Simiantonakis, J., Huber, P., and Brix, G. Quantitative MR temperature monitoring of high intensity focused ultrasound therapy. Magn. Reson. Imaging, *17:* 603–610, 1999.
22. Bohris, C., Jenne, J. W., Rastert, R., Simiantonakis, I., Brix, G., Spoo, J., Hlavac, M., Nemeth, R., Huber, P. E., and Debus, J. MR monitoring of focused ultrasound surgery (FUS) in a breast tissue model. Magn. Reson. Imaging, *19:* 167–175, 2001.
23. Chen, L., Bouley, D., Yuh, E., D'Arcueil, H., and Butts, K. Study of focused ultrasound tissue damage using MRI and histology. J. Magn. Reson. Imaging, *10:* 146–153, 1999.
24. Salomir, R. S., Vimieux, F. C., de Zwart, J. A., Grenier, N., and Moonen, C. T. W. Hyperthermia by MR guided focused ultrasound: accurate temperature control based on fast MRI and a physical model of local energy deposit and heat conduction. Magn. Reson. Med., *43:* 342–347, 2000.
25. McDannold, N. J., King, R. L., Jolesz, J. A., and Hynynen, K. Usefulness of MR imaging derived thermometry and dosimetry in determining the threshold for tissue damage induced by thermal surgery in rabbits. Radiology, *216:* 517–523, 2000.
26. Hynynen, K., Pomeroy, O., Smith, D. N., Huber, P. E., McDannold, N., Kettenbach, J., Baum, J., Singer, S., and Jolesz, F. A. MRI guided focused ultrasound surgery (FUS) of fibroadenomas in the breast. Radiology, *219:* 176–185, 2001.
27. Elston, C. W., and Ellis, I. O. Pathological prognostic factors in breast cancer. I. The value of histological grade in breast cancer: experience from a large study with long-term follow-up. Histopathology, *19:* 403–410, 1991.
28. Sinn, H. P., Anton, H. W., Oelmann, A., Bastert, G., and Otto, H. F. Relationship between Invasive and non-invasive carcinoma and the risk of intramammary recurrences after breast-conserving therapy. Eur. J. Cancer, *34:* 646–653, 1998.
29. Gamarra, F., Spelsberg, F., Kuhnle, G. E., Mueller-Klieser, W., and Goetz, A. E. High energy shock waves induce blood flow reduction in tumors. Cancer Res., *53:* 1590–1595, 1993.
30. Debus, J., Spoo, J., Jenne, J., Huber P., and Peschke, P. Sonochemically induced radicals generated by pulsed high-energy ultrasound *in vitro* and *in vivo*. Ultrasound Med. Biol., *25:* 301–306, 1999.
31. Huber, P., Peschke, P., Brix, G., Hahn, E. W., Lorenz, A., Tiefenbacher, U., Wannenmacher, M., and Debus, J. Synergistic interaction of ultrasonic shock waves and hyperthermia in the Dunning prostate tumor R3327-AT1. Int. J. Cancer, *82:* 84–91, 1999.
32. Huber, P. E., and Debus, J. Tumor cytotoxicity *in vivo* and radical formation *in vitro* are dependent on shock wave-induced cavitation dose. Radiat. Res., *156:* 301–309, 2001.
33. Ashush, H., Rozenszajn, L. A., Blass, M., Barda-Saad, M., Azimov, D., Radnay, J., Zipori, D., and Rosenschein, U. Apoptosis induction of human myeloid leukemic cells by ultrasound exposure. Cancer Res., *4:* 1014–1020, 2000.
34. Vykhodtseva, N., McDannold, N., Martin, H., Bronson, R. T., and Hynynen, K. Apoptosis in ultrasound-produced threshold lesions in the rabbit brain. Ultrasound Med. Biol, *27:* 111–117, 2001.
35. Delius, M., and Adams, G. Shock wave permeabilization with ribosome inactivating proteins: a new approach to tumor therapy. Cancer Res., *59:* 5227–5232, 1999.
36. Huber, P. E., and Pfisterer, P. *In vitro* and *in vivo* transfection of plasmid DNA in the Dunning prostate tumor R3327-AT1 is enhanced by focused ultrasound. Gene Ther., *7:* 1516–1525, 2000.
37. Fisher, B., Brown, A., Mamounas, E., Wieand, S., Robidoux, A., Margolese, R. G., Cruz, A. B. Jr., Fisher, E. R., Wickerham, D. L., Wolmark, N., DeCillis, A., Hoehn, J. L., Lees, A. W., and Dimitrov, N. V. Effect of preoperative chemotherapy on local-regional disease in women with operable breast cancer: findings from National Surgical Adjuvant Breast and Bowel Project B-18. J. Clin. Oncol., *15:* 2483–2493, 1997.
38. Mamounas, E. P., and Fisher, B. Preoperative chemotherapy for operable breast cancer. Cancer Treat. Res., *103:* 137–155, 2000.
39. Fisher, B., Dignam, J., Tan-Chiu, E., Anderson, S., Fisher, E. R., Wittliff, J. L., and Wolmark, N. Prognosis and treatment of patients with breast tumors of one centimeter or less and negative axillary lymph nodes. J. Natl. Cancer Inst. (Bethesda), *17:* 112–120, 2001.

40. Mumtaz, H., Hall-Craggs, M. A., Wotherspoon, A., Paley, M., Buonaccorsi, G., Amin, Z., Wilkinson, I., Kissin, M. W., Davidson, T. I., Taylor, I., and Bown, S. G. Laser therapy for breast cancer: MR imaging and histopathologic correlation. Radiology, *200:* 651–658, 1996.
41. Milne, P. J., Parel, J. M., Manns, F., Denham, D. B., Gonzalez-Cirre, X., and Robinson, D. S. Development of stereotactically guided laser interstitial thermotherapy of breast cancer: *in situ* measurement and analysis of the temperature field in *ex vivo* and *in vivo* adipose tissue. Lasers Surg. Med., *26:* 67–75, 1998.
42. Rui, J., Tatsutani, K. N., Dahiya, R., and Rubinsky, B. Effect of thermal variables on human breast cancer in cryosurgery. Breast Cancer Res. Treat., *53:* 185–192, 1999.
43. Weissleder, R., Tung, C. H., Mahomood, U., and Bogdanov, A. Jr. *In vivo* imaging of tumors with protease-activated near-infrared fluorescent probes. Nat. Biotechnol., *17:* 375–378, 1999.
44. Shangvi, N. T., Hynynen, K., and Lizzi, F. L. New developments in therapeutic ultrasound. IEEE Trans. Biomed. Eng., *15:* 83–92, 1996.
45. Wan, H., VanBaren, P., Ebbini, E. S., and Cain, C. A. Ultrasound surgery: comparison of strategies using phased array systems. IEEE Trans. Ultrason. Ferroelectr. Freq. Contr., *43:* 1085–1098, 1996.
46. Daum, D. R., Smith, N. B., King, R., and Hynynen, K. In vivo demonstration of noninvasive thermal surgery of the liver and kidney using ultrasonic phased array. Ultrasound. Med. Biol., *25:* 1087–1098, 1999.